Journal of Inflammation Research

Dovepress
Taylor & Francis Group

Open Access Full Text Article

ORIGINAL RESEARCH

GPX3 as a Novel and Potential Therapeutic Target in the Shared Molecular Mechanisms of Traumatic Brain Injury and Parkinson's Disease

Yue Wang[1–5], Jiang Fang[1–5], Qiang Yuan[1–5], Jian Yu[1–5], Jin Hu[1–5]

[1]Department of Neurosurgery, Huashan Hospital, Fudan University, Shanghai, 200040, People's Republic of China; [2]National Center for Neurological Disorders, Huashan Hospital, Fudan University, Shanghai, 200040, People's Republic of China; [3]Shanghai Key Laboratory of Brain Function and Restoration and Neural Regeneration, Huashan Hospital, Fudan University, Shanghai, 200040, People's Republic of China; [4]Neurosurgical Institute of Fudan University, Huashan Hospital, Fudan University, Shanghai, 200040, People's Republic of China; [5]Shanghai Clinical Medical Center of Neurosurgery, Huashan Hospital, Fudan University, Shanghai, 200040, People's Republic of China

Correspondence: Jian Yu; Jin Hu, Department of Neurosurgery, Huashan Hospital, Fudan University, 12 Wulumuqi Zhong Road, Shanghai, 200040, People's Republic of China, Tel +86 21 52889999, Email hujin@fudan.edu.cn; lance2000@hotmail.com

Background: Traumatic brain injury (TBI) is a prevalent neurological disorder associated with significant public health burdens and long-term risks, including neurodegenerative diseases such as Parkinson's disease (PD). Emerging evidence suggests a strong link between moderate to severe TBI and an elevated risk of PD, though the underlying mechanisms remain poorly understood.

Materials and Methods: Common differentially expressed genes (DEGs) were identified in GEO datasets of patients with traumatic brain injury (TBI) and Parkinson's disease (PD). Further analyses, including GO and KEGG pathway enrichment, protein-protein interaction (PPI) network construction, hub gene identification, as well as miRNA and transcription factor prediction and drug candidate screening, were conducted. Subsequently, the expression of hub genes was validated using additional TBI- and PD-related GEO datasets and the Comparative Toxicogenomics Database (CTD). Finally, the expression of hub genes was further validated in a mouse model of TBI induced by controlled cortical impact (CCI).

Results: Shared transcriptional signatures between TBI and PD were uncovered, highlighting overlapping molecular networks and pathways. The glutathione peroxidase 3 (GPX3) gene emerged as a pivotal hub gene, with its expression significantly altered in both TBI and PD datasets.

Conclusion: This study underscores the critical role of GPX3 in the molecular intersection of TBI and PD, suggesting it as a novel and potential therapeutic target, offering new insights into potential therapeutic strategies.

Keywords: traumatic brain injury, Parkinson's disease, bioinformatics, oxidative stress, mitochondrial dysfunction, neurodegenerative diseases

Introduction

Traumatic brain injury (TBI) has the highest incidence rate among common neurological disorders and represents a significant public health burden.[1–3] It is also a leading cause of neurological disability, with a substantial risk of neurological and neuropsychiatric complications, including in cases classified as mild or moderate.[4] Increasingly, TBI is recognized not only as an acute condition but also as a chronic disease with long-term consequences, including a heightened risk of late-onset neurodegenerative disorders.[5,6] Parkinson's disease (PD) is the second most prevalent neurodegenerative disorder, affecting 2–3% of the population over the age of 65, with its prevalence projected to double by 2050.[7,8] PD is currently described as a multisystem neurodegenerative disorder, simultaneously impacting the central nervous system (CNS), enteric nervous system (ENS), autonomic nervous system, adaptive immune system, and gastrointestinal (GI) tract. Clinically, it is characterized by a spectrum of motor and non-motor symptoms.[9] The relationship between TBI and PD has garnered increasing attention, particularly in cases of moderate to severe TBI, which have been identified as a risk factor for all-cause dementia and Parkinson's disease.[10–12] Two of the largest

Received: 17 November 2024
Accepted: 29 January 2025
Published: 7 February 2025

administrative and population-based cohort studies to date reported that the risk of clinical Parkinson's disease (PD) is at least 1.8 times greater in individuals with a history of moderate/severe traumatic brain injury (TBI) compared to those without TBI, with an average follow-up of 4.6 years, after adjusting for various demographic, medical, and psychiatric factors.[13,14]

However, the mechanisms underlying the increased risk of Parkinson's disease following TBI remain poorly understood. Reactive oxygen species (ROS) are chemically reactive molecules, including free radicals such as superoxide ($O_2\bullet^-$) and hydroxyl (•OH), and non-radicals such as hydrogen peroxide (H_2O_2) and singlet oxygen ($^1O_2$), all derived from molecular oxygen. At low levels, ROS play a key role in regulating normal physiological processes, including the activation of the innate immune system.[15,16] ROS not only cause DNA damage and drive tumorigenesis but also accelerate its progression.[15,17,18] Elevated levels of H_2O_2 can trigger cell cycle arrest or apoptosis. Certain anticancer agents act by generating ROS, which induce cell death through apoptotic signaling pathways.[18] However, at excessively high pathological levels, ROS contribute to the development of cardiovascular diseases and other conditions.[17,19,20] The cellular system relies on antioxidant enzymes as its first line of defense against ROS. Glutathione peroxidase (GPX), an essential enzyme, plays a crucial role in the detoxification of hydrogen peroxide. Within cells, hydrogen peroxide is catalyzed by catalases and GPX into water.[21,22] Glutathione Peroxidases, discovered by Gordon C. Mills in 1957, are a family of enzymes vital for the removal of hydrogen peroxide generated endogenously.[19,23] They also catalyze the conversion of glutathione (GSH) to its oxidized form, glutathione disulfide(GSSG)[21]. Among the reported GPxs, GPx3 is a homotetramer that can eliminate a wide range of complex hydroperoxides. Beyond its roles in the cytosol and mitochondria, GPx3 also circulates in plasma.[24] GPx3 presence helps mitigate inflammation within the tumor microenvironment.[25] Additionally, reduced GPx3 protein levels have been observed in inflammatory breast cancer.[26] However, there is a paucity of research on GPX3 in the contexts of traumatic brain injury and Parkinson's disease.

In recent years, advancements in bioinformatics and the use of genomic microarrays have made bioinformatics analysis an indispensable tool in biomedical research. Common transcriptional patterns can offer new insights into the shared etiology of TBI and PD. In this study, we obtained two key microarray datasets (GSE104687, GSE7621) from the GEO database. The two GEO datasets utilized in the initial analysis are derived from human brain samples of traumatic brain injury (TBI) and Parkinson's disease (PD), offering greater reliability and translational potential compared to the mouse-derived GEO datasets.

We conducted comprehensive bioinformatics and enrichment analyses to identify differentially expressed genes and their functions in TBI and PD. Based on these analyses, we identified a shared profile of genes, molecular networks, and signaling pathways between TBI and PD, with key genes in these profiles subsequently validated.

Materials and Methods

Data Download

The TBI dataset (GSE104687) was retrieved from the NCBI GEO public database.[27] This dataset includes 376 samples from 107 brains, encompassing cortical grey matter, white matter, and hippocampal tissue. The GSE7621 dataset, associated with Parkinson's disease, was also downloaded, containing a total of 64 transcriptomic datasets, with 9 from normal samples and 16 from Parkinson's disease samples.[28] The quality control and batch correction were performed using the PCA function and the ComBat function from the sva R package(version 3.52.0).

Differentially expressed genes (DEGs) were identified using the limma R package(version 3.60.4), with the screening criteria set as p-value < 0.05 and |logFC| > 1. Additionally, the GSE150696 and GSE155063 datasets were downloaded as validation sets for the identified hub genes.[29,30]

GO and KEGG Enrichment Analysis

The DEGs were then analyzed using Gene Ontology (GO) and Kyoto Encyclopedia of Genes and Genomes (KEGG) pathway analysis to identify the biological functions and signaling pathways involved in disease onset and progression.[31,32] In the enrichment analysis, FDR is used to correct the results, and $p < 0.05$ is considered significant.

Network Analysis and Hub Genes Identification

The common differentially expressed genes (DEGs) were used to construct the protein-protein interaction (PPI) network via the STRING database (https://string-db.org/),[33] with results visualized using Cytoscape (version 3.10.1). Hub genes and essential networks were identified using the CytoHubba plugins in Cytoscape. CytoHubba is a plugin used to identify and prioritize hub genes within a network based on various centrality measures, such as degree, closeness, and betweenness centrality. It helps to highlight the most influential genes in biological networks, which may be critical for understanding cellular processes or disease mechanisms.

Additionally, the GeneMANIA database (https://genemania.org/) was employed to analyze the gene network of the identified hub genes.[34] GeneMANIA is valuable for identifying gene interactions, understanding gene functions, and prioritizing genes for further study. It is particularly useful for exploring pathways in disease research and biomarker discovery. In this study, NetworkAnalyst 3.0 was utilized to identify the TF-gene network and the TF-miRNA co-regulatory network.[35]

Obtainment of Potential Key Genes for Traumatic Brain Injury and Parkinson's Disease

The Comparative Toxicogenomics Database (CTD, http://ctdbase.org/) provides data on interfaces between chemicals, genetic products, biological outcomes, and diseases and contributes to the study of potential mechanisms of pharmaceutical action and disease-related environmental exposures.[36] Using the CTD database, the associations between hub genes and the risk of the onset of brain injury, Parkinson's disease, neurodegenerative diseases, were analyzed.

Potential Therapeutic Drugs Associated With Hub Genes

A The Connectivity Map (CMap) database (https://clue.io/) is a promising tool for drug screening, capable of predicting molecularly targeted drugs based on differential gene expression (DEG).[37] The CMap database uses cell expression profile data, which has been processed with 164 drugs and small molecule compounds, along with overexpression or gene knockout tools. It utilizes the L1000 analysis platform to investigate the relationships among drugs, small molecules, genes, and disease states. In this study, we leveraged gene expression profiling in conjunction with the CMap database to predict potential chemical drugs for treating traumatic brain injury (TBI) and Parkinson's disease (PD). Our findings suggested that targeting the functions of specific genes could offer therapeutic benefits. Notably, the expression profiles of these genes were found to be the inverse of the disease's characteristic expression profiles, with negative enrichment scores indicating a potential therapeutic effect.

Single-Cell Sequencing Dataset Analysis

The GSE269748 dataset, which pertains to traumatic brain injury (TBI), was utilized for this study. Data from day 7 post-TBI were selected for analysis. This single-cell dataset contains 10,312 cells. Initially, the dataset was processed using the Seurat package(version 5.1.0), followed by t-SNE analysis to visualize the spatial relationships between different cell clusters.[38] A final resolution of 0.4 was chosen after evaluating cluster stability, clustering patterns, and the top marker genes. Marker genes for each cell subtype were identified through the FindAllMarkers function, which enabled the extraction of relevant gene profiles from the single-cell expression data. Finally, cell type annotation was performed using the GPTCelltype R package(version 1.0.1),[39] which helped in categorizing the different cell populations in the dataset.

Animals and Experimental Design

Adult male C57BL/6 mice (8–10 weeks old, weighing 23–27 grams) were obtained from Shanghai Jihui Laboratory Animal Care Co., Ltd. The mice were housed under pathogen-free conditions in individually ventilated cages (IVC), with a stable and controlled environment maintaining appropriate temperature and humidity levels. A 12-hour light–dark cycle was observed, and mice had ad libitum access to both food and water. Prior to experimentation, the mice were allowed to acclimate to their environment for a minimum of 3 days. The study was approved by the Animal Ethics Committee of the Department of Laboratory Animal Science, Fudan University (Approval number: 2021JS −342). Mice were randomly

assigned to two groups: the sham-operated group (sham) and the traumatic brain injury (TBI) group. The sham group underwent a mock surgery, while the TBI group underwent the traumatic brain injury modeling procedure.

In the CCI model, the sample size for the TBI group and the sham group is 4. Humane care was provided for all animals in accordance with the criteria described in the Guide for the Care and Use of Laboratory Animals (National Institutes of Health publication 86–23, revised 2011).

Mouse Model of Traumatic Brain Injury

The traumatic brain injury (TBI) mouse model was induced using a controlled cortical impact (CCI) technique as previously described.[40] This model generally avoids postoperative mortality in mice. Mice were anesthetized, positioned securely, and their skulls were exposed. The site for CCI was marked 2 mm lateral to the midline and 0.5 mm posterior to the bregma. A consistent right-side craniotomy was performed using a skull drill to create a cranial window approximately 4 mm in diameter. The brain tissue was impacted using a cortical impactor device (TBI 0310, Precision Systems and Instrumentation) fitted with a 3 mm flat-tip impactor head, following specified parameters: a velocity of 3.5 m/s, an impact depth of 1.5 mm, and a duration of 150 ms. Following the CCI procedure, the scalp was carefully sutured, disinfected, and the mice were placed on a heating pad to stabilize body temperature until they had fully emerged from anesthesia. Mice in the sham group received the same surgical procedures except for the CCI.

Immunofluorescence

Anesthetized mice were transcardially perfused with PBS and 4% paraformaldehyde to fix the brain tissue. The brains were then immersed in 4% paraformaldehyde and 20% and 30% sucrose solutions for fixation and dehydration. Coronal sections of 25 μm were cut using a freezing microtome (HM525NX, ThermoFisher, USA). The sections were washed and blocked with 10% goat or donkey serum for 1 hour.Subsequently, the brain sections were incubated overnight at 4°C with the following primary antibodies: anti-Gpx3 (1:1000, ab256470, abcam) and anti-Iba1 (1:1000, ab283346, abcam). The next day, after washing, fluorescently labeled secondary antibodies were added: Goat Anti-Rabbit IgG H&L (Alexa Fluor® 594, ab150080, 1:200, abcam) and Goat Anti-Rat IgG H&L (Alexa Fluor® 647, ab150159, 1:200, abcam), and incubated in the dark for 1 hour at room temperature. Finally, the sections were washed three times, and DAPI was added to stain the nuclei, followed by observation under a fluorescence microscope.

For quantification of relative fluorescent intensity in individual neurons, all images were acquired using the same parameters (laser power and pinhole sizes). Images were first exported from the NIS-Elements Viewer 5.21 (Zeiss) as tif and then processed in ImageJ. The antibodies used have been validated in mice. The obtained immunofluorescence images were quantitatively analyzed using ImageJ, with the average fluorescence intensity of the sham group used as the normalization reference. Immunofluorescence images were quantitatively analyzed using ImageJ, normalizing the results to the average fluorescence intensity of the sham group.

Statistical Analysis

Statistical analysis was carried out using R language (version 4.4) and GraphPad Prism (version 3.10.1). Statistical analysis was performed based on the normality and homogeneity of variance of the measurement data. For two groups, either the unpaired *t*-test or the Mann–Whitney *U*-test was employed, while for multiple groups, One-way analysis of variance (ANOVA) or the Kruskal–Wallis test was used. All statistical tests were two-sided at a significance threshold of 0.05.

Results

Identification of DEGs in GSE104687 and GSE7621

The workflow of this study is shown in Figure 1. Utilizing data from the NCBI GEO database, we obtained the Series Matrix File for GSE104687, which focuses on traumatic brain injury. This dataset includes 376 samples from 107 individual brains, encompassing cortical grey matter, white matter, and the hippocampus. Differentially expressed genes (DEGs) between the two sample groups were identified using the limma package, with a significance threshold of a p-value < 0.05 and $|\log FC| > 1$.

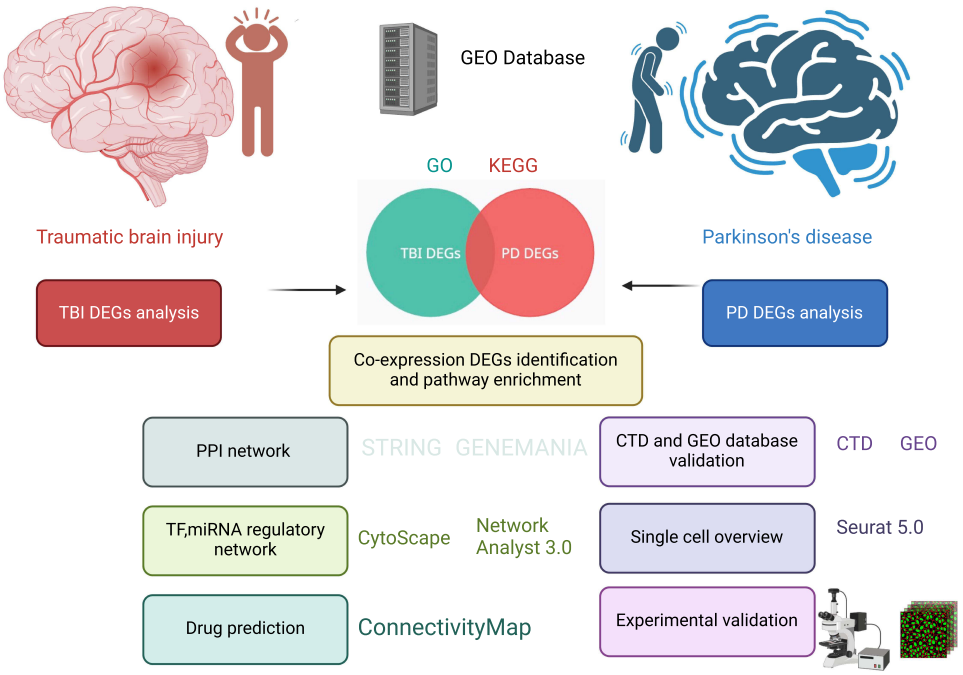

Figure 1 Study flowchart. Created in BioRender. Y, (W) (2024) https://BioRender.com/r08a794.

A total of 912 DEGs were identified, including 474 upregulated and 438 downregulated genes (Figure 2A and C). Next, we obtained the Series Matrix File for GSE7621, related to Parkinson's disease. This dataset comprised 64 transcriptome samples: 9 from normal controls and 16 from PD patients. The limma program was again employed to calculate differences between the groups, yielding a total of 718 DEGs—319 upregulated and 399 downregulated—under the conditions of a p-value threshold of < 0.05 and $|\log FC| > 1$ (Figure 2B and D).

GO and KEGG Enrichment Analysis of DEGs in TBI and PD

We conducted a pathway enrichment analysis on the DEGs from these two datasets. The findings revealed that the 912 DEGs in GSE104687 were primarily enriched in ribosomal pathways, mitochondrial activation, amino acid metabolism, and pathways associated with neurodegenerative diseases (Figure 3A–C). The 718 DEGs of GSE7621 were mainly enriched in pathways linked to neuronal activity, mitochondrial activation, immune cell infiltration and differentiation, as well as the PI3K-Akt signaling pathway (Figure 3D–F).

Identification and Pathway Analysis of Co-Expressed DEGs in TBI and PD

These differentially expressed genes (DEGs) were analyzed using a Venn diagram, with exclusion of DEGs exhibiting opposite expression trends, resulting in a total of 20 common DEGs identified (Figure 4A–C), including 10 upregulated and 10 downregulated genes.

The ten upregulated genes identified are ANGPT2, COL9A1, CREBBP, NCF4, CXCR4, MAFF, CLDN15, NPHP3, PLCXD1, and TEX29. The ten downregulated genes identified are DCC, GPX3, HBA2, RBM3, EBP, PITHD1, SLC12A8, RERG, DPH6, and C2orf80.

The upregulated genes were primarily enriched in hypoxia-related pathways, with CXCR4, CREBBP, and ANGPT2 playing key roles (Figure 4D). In contrast, the downregulated genes were mainly enriched in pathways related to hydrogen peroxide catabolism, hydrogen peroxide metabolism, and cellular oxidant detoxification, with GPX3 and HBA2 serving as key contributors to these pathways (Figure 4E and F).

https://doi.org/10.2147/JIR.S506891

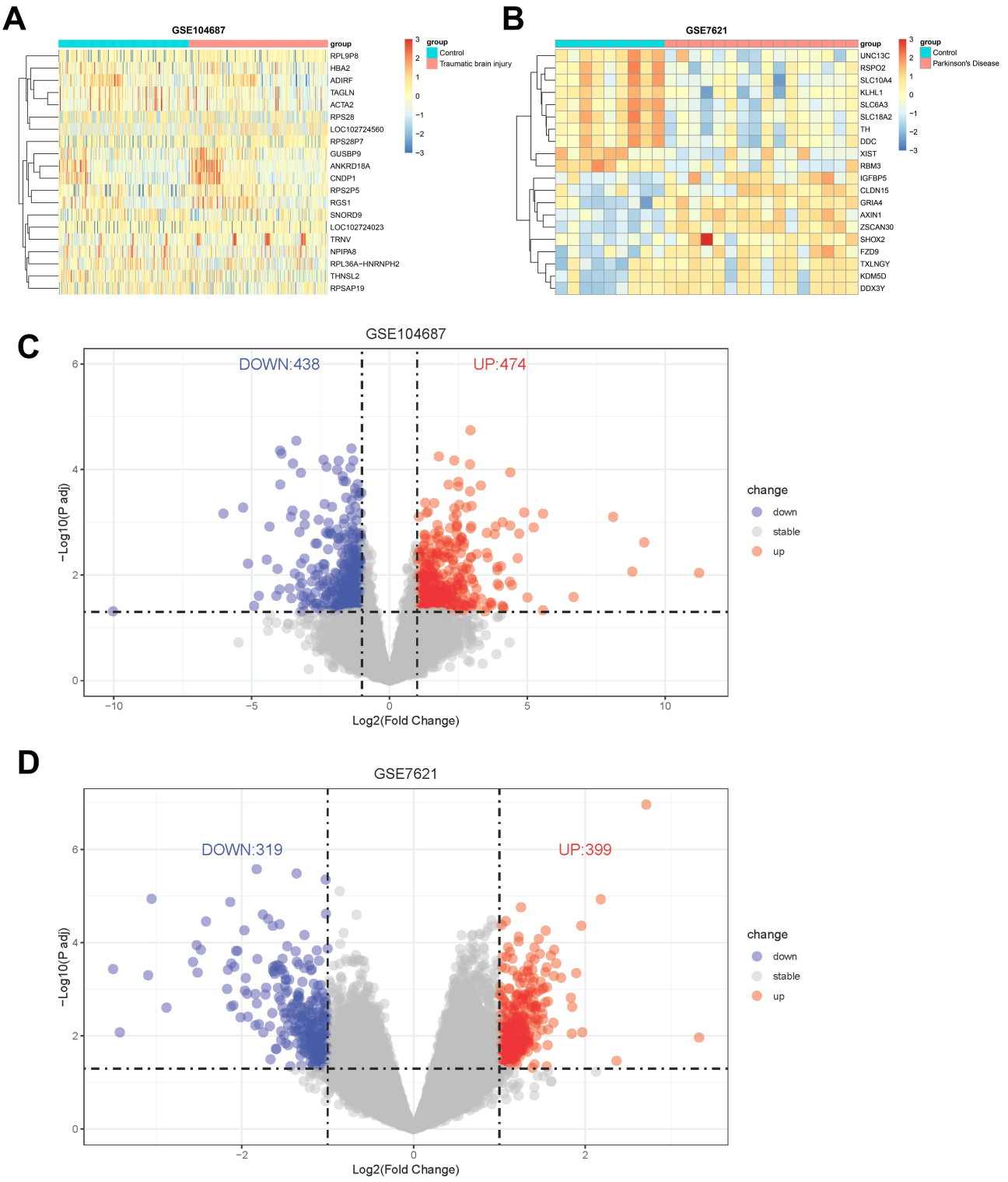

Figure 2 Identification of DEGs in GSE104687 and GSE7621. (**A**) Heatmap of DEGs in TBI(GSE104687). (**B**) Heatmap of DEGs in PD(GSE7621). (**C**)Volcano map DEGs in TBI(GSE104687). (**D**)Volcano map of DEGs in PD(GSE7621).

Protein-Protein Interaction Network Analysis and Hub Gene Identification

The 20 common DEGs were inputted into STRING to construct the PPI network, and the generated file was imported into Cytoscape for visualization (Figure 5A and B). The cytoNCA plugin was used to identify key genes within

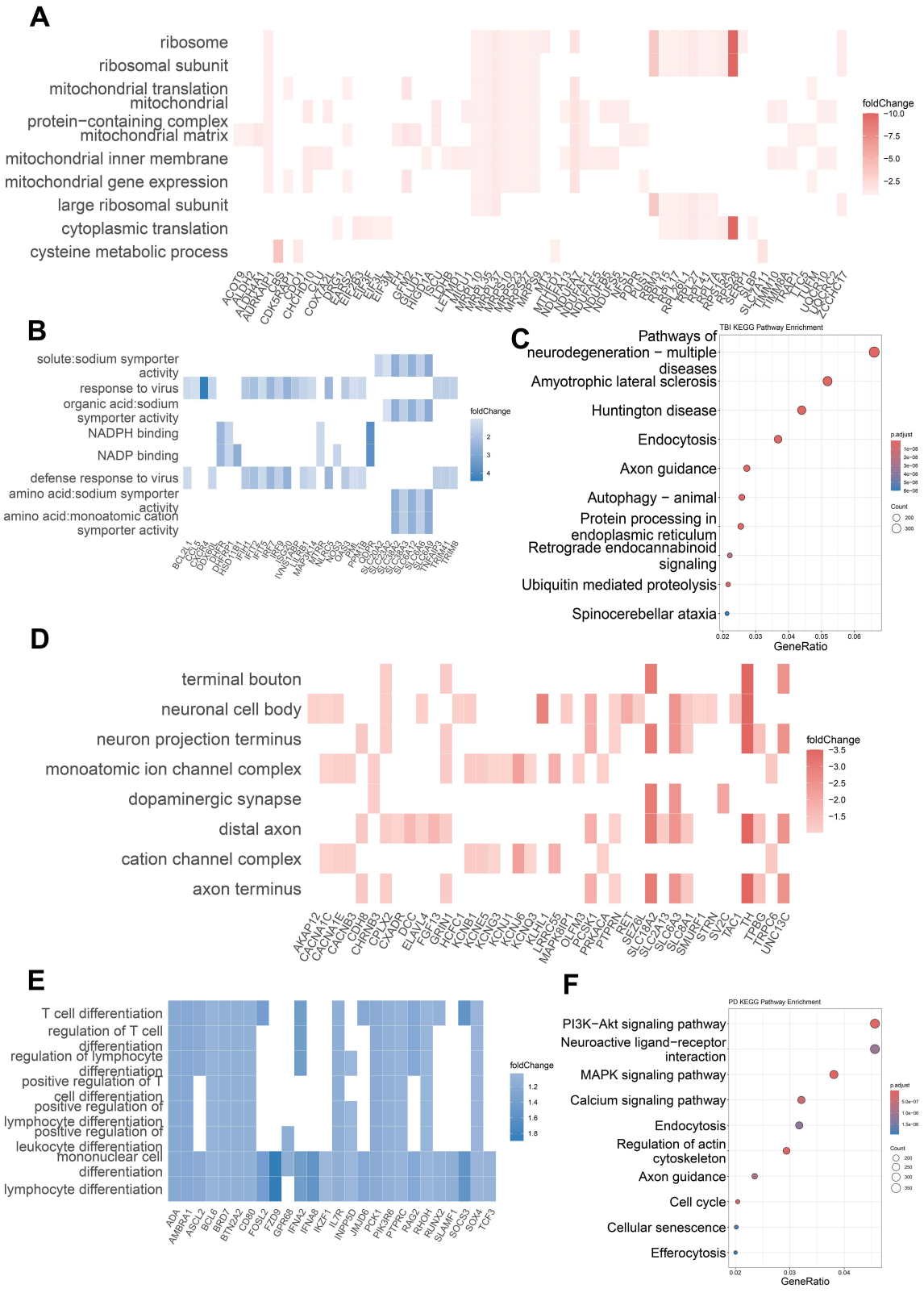

Figure 3 GO and KEGG enrichment pathway analysis of TBI and PD DEGs. (**A**) Heatmap of GO pathways enriched in GSE104687 downregulated genes. (**B**) Heatmap of GO pathways enriched in GSE104687 upregulated genes. (**C**) Dotplot of KEGG pathways enriched in GSE104687 DEGs. (**D**) Heatmap of GO pathways enriched in GSE7621 downregulated genes. (**E**) Heatmap of GO pathways enriched in GSE7621upregulated genes. (**F**) Dotplot of KEGG pathways enriched in GSE7621 DEGs. In the GO enrichment analysis heatmap, rows represent different cellular structures or pathways, columns represent different genes, and colors indicate the fold change of gene expression.

https://doi.org/10.2147/JIR.S506891

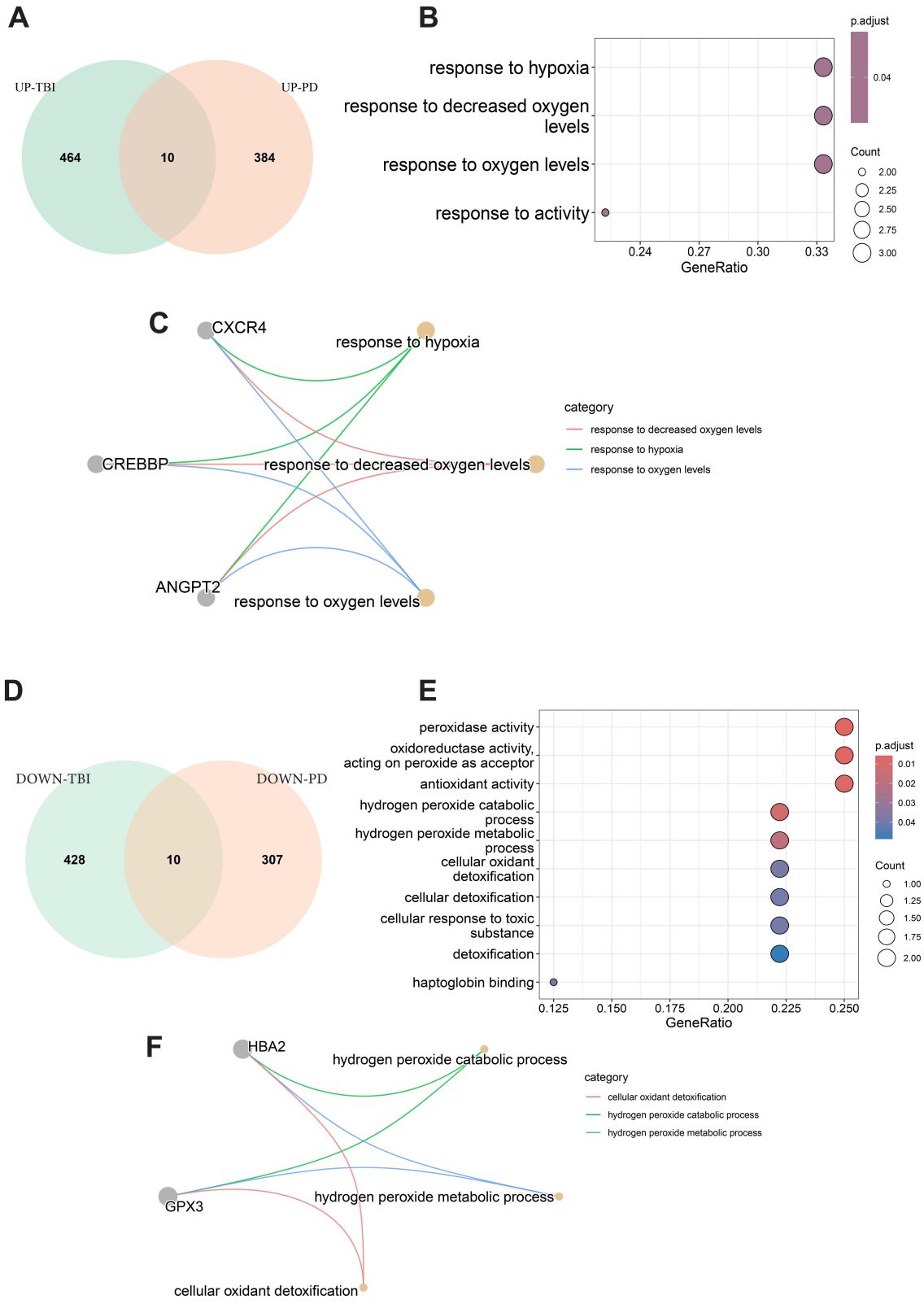

Figure 4 Identification and pathway analysis of co-expressed DEGs in GSE104687 and GSE7621. (**A**)Venn diagrams identify co-upregulated genes in GSE104687 and GSE7621. (**B**) KEGG enrichment pathways enriched in co-upregulated genes. (**C**) GO Enrichment network of co-upregulated genes. (**D**)Venn diagrams identify co-downregulated genes in GSE104687 and GSE7621. (**E**) KEGG enrichment pathways enriched in co-downregulated genes. (**F**) GO Enrichment network of co-downregulated genes.

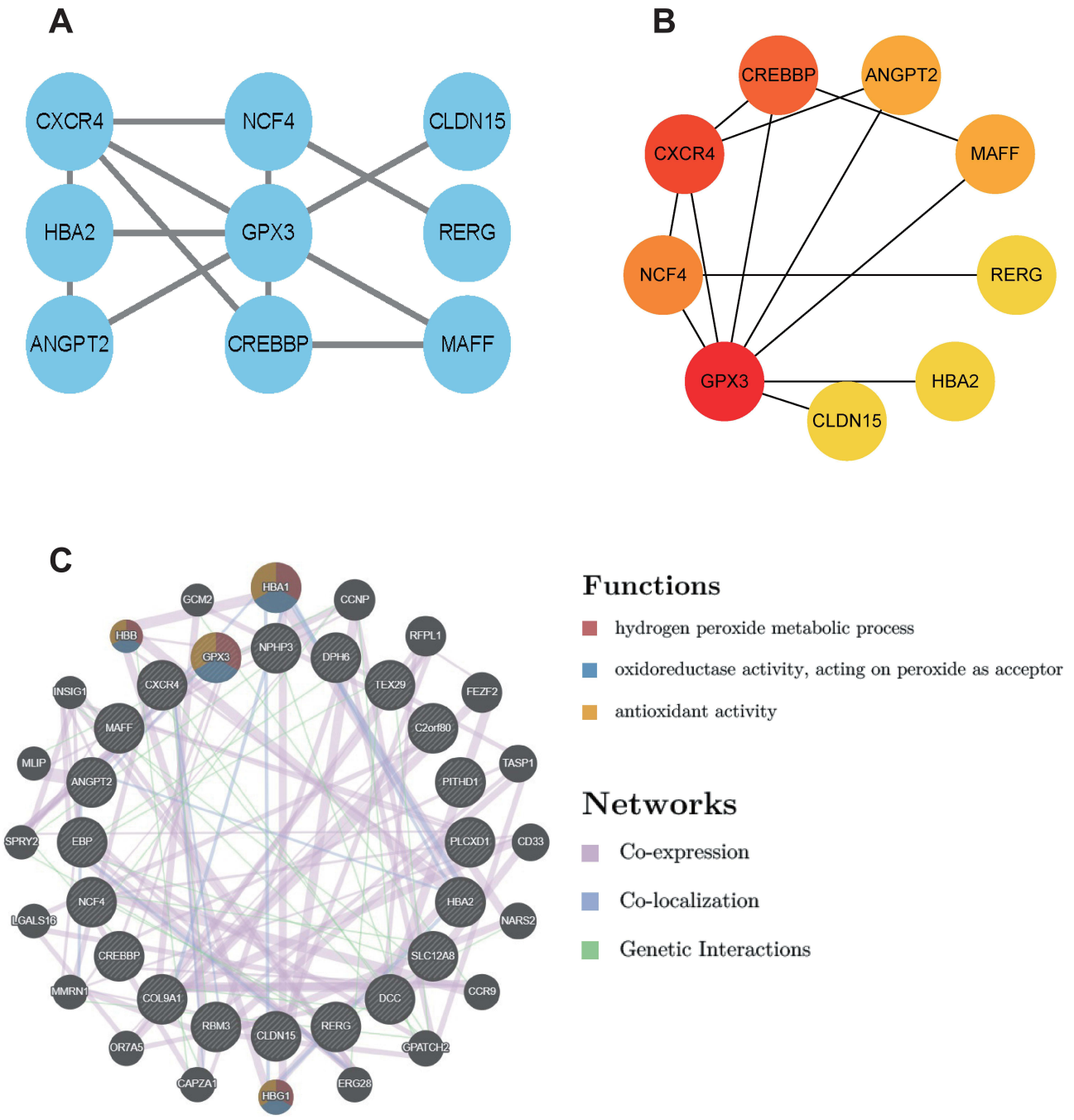

Figure 5 Protein-Protein Interaction (PPI) Network Analysis and Hub Gene Identification. (**A**) PPI network for common DEGs shared by TBI and PD. Blue nodes represent shared DEGs. (**B**) A key cluster of 15 genes was selected using the CytoNCA plugin in Cytoscape. The color of each node represents its Subgraph Centrality, with larger values represented by red and smaller values by yellow.(**C**) Gene network and functional analysis of hub genes were performed using GeneMANIA. The inner circle represents hub genes, while the outer circle represents the corresponding reciprocal genes. Colors of nodes represent gene function annotations, corresponding to GO terms enriched in the network. Edge colors represent interactions based on co-expression, physical interactions, co-localization, shared protein domains, or predicted interactions.

a subnetwork consisting of 9 nodes and 12 edges, as depicted in Figure 4. The genes involved in this module were GPX3, NCF4, CXCR4, CREBBP, ANGPT2, MAFF, RERG, HBA2, and CLDN15. GeneMANIA was utilized to construct an extended gene network. Gene functional annotation revealed that these hub genes are associated with hydrogen peroxide metabolism, oxidoreductase activity, and antioxidant function (Figure 5C).

https://doi.org/10.2147/JIR.S506891

Transcription Factor-Hub Gene Network and miRNA-Hub Gene Coregulatory Network

The identification of common DEGs in the TF-gene and TF-miRNA co-regulatory networks was carried out using NetworkAnalyst 3.0. This network consists of 8 seeds, 145 nodes, and 180 edges (Figure 6A). The betweenness of each node was calculated using CytoHubba, resulting in a network of the top 20 nodes ranked by betweenness (Figure 6B). Within the network of TF-gene interactions, GPX3, MAFF, and CLDN15 exhibited extensive connections with other transcription factors (TFs). Among the TFs, WRNA1, ZFP37, and IKZF1 demonstrated the highest activity within the TF-gene interaction network. Subsequently, we constructed a TF-miRNA coregulatory network to predict interactions among shared DEGs, TFs, and miRNAs. The miRNAs most closely associated with TFs and hub genes are miR-548-3p, miR-653, miR-543, and miR-340 (Figure 6C).

Prediction of Candidate Drugs for TBI-Related Parkinson's Disease

To identify potential therapeutic agents for TBI-related Parkinson's disease, the 20 hub DEGs and associated transcription factors were submitted to the cMAP database. Drug candidates were ranked by absolute enrichment score (Table 1). The analysis showed that Necrostatin-1, JTE-907, rhapontin, rucaparib, nimetazepam, RHO-kinase inhibitor III, HA-14-1, liothyronine, alimemazine, and PD-173074 were the top 10 candidate drugs. These agents represent promising candidates for the treatment of TBI-related Parkinson's disease.

Dataset Validation of Hub Genes

The Comparative Toxicogenomics Database (CTD) is a resource that explores relationships between genes, diseases, and environmental chemicals, providing curated data on gene-chemical and gene-disease interactions. The CTD database was used to analyze associations between hub DEGs and conditions like brain injury, Parkinson's disease, and other neurodegenerative diseases. The results demonstrated that GPX3, CXCR4, CREBBP, and ANGPT2 had the strongest association with brain injury, while GPX3 showed the highest correlation with Parkinson's disease and other neurodegenerative diseases (Figure 7A).

To further validate the hub genes, we used four CytoHubba algorithms (MCC, MNC, degree, and betweenness) in Cytoscape and confirmed them using the GEO database. Through Venn diagram analysis, we found that GPX3, CXCR4, and CREBBP consistently ranked in the top five across all four algorithms (Figure 7B).

We analyzed the mouse TBI dataset GSE150696. Results indicated significant differences in the expression levels of Gpx3 and Crebbp between the injured and uninjured hemispheres of TBI mice (Figure 7C–E). For validation in human Parkinson's disease, we used the GSE155063 dataset, where GPX3 and CXCR4 expression levels were significantly altered compared to the control group (Figure 7F–H).

In summary, GPX3 emerged as the top-performing gene, both in terms of CTD database scores and validation within the GEO dataset.

Overview of Gpx3 Expression in Single-Cell RNA-Seq Dataset and Experimental Validation of Gpx3

We obtained the single-cell dataset GSM8326363 from GSE269748, which is derived from the cortex of a mouse on day 7 post-TBI. Single-cell analysis was performed using the Seurat package, with T-SNE used for visualization. Clusters were annotated with the GPTcelltype R package, categorizing cells into eight types: endothelial cells, microglia, macrophages, ependymal cells, NK and T cells, glial cells, neutrophils, and monocytes (Figure 8A and B). Expression levels of Gpx3 across these cell types are shown in Figure 8C.

We performed immunofluorescence experiments on brain tissues from the sham group and mice at days 4 and 14 post-TBI, and quantified the immunofluorescence intensity of Gpx3 (Figure 8D). This experiment revealed GPX3 expression and localization in the cortex after TBI. In the merged images, GPX3 largely co-localizes with IBA1-positive cells in the TBI group, indicating decreased GPX3 expression in microglia and macrophages following TBI (Figure 8E).

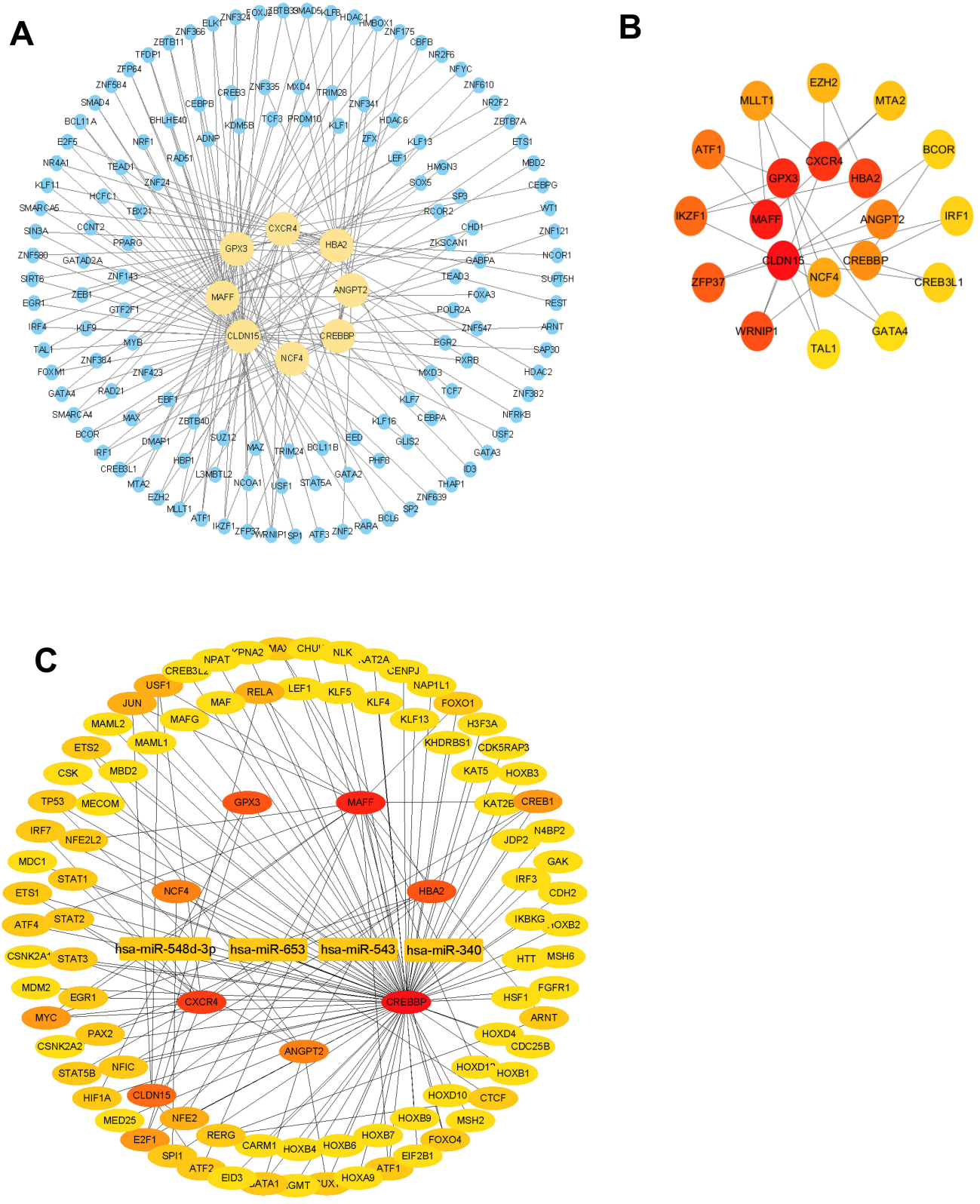

Figure 6 Transcription Factor-Hub Gene Network and miRNA-Hub Gene Coregulatory Network. (**A**) Transcription Factor-Hub Gene Network. (**B**) The TF-hub gene network consists of the top 20 nodes ranked by betweenness values calculated using the CytoHubba plugin. The inner circle represents hub genes, while the outer circle represents TFs, with more yellow indicating higher betweenness values. (**C**) miRNA-Hub Gene Coregulatory Network. The inner circle represents hub miRNAs, with more yellow indicating higher betweenness values.

https://doi.org/10.2147/JIR.S506891

Table 1 Candidate Drugs Predicted With the Common Hub Genes

Rank	Score	Name	Description
1	−96.86	Necrostatin-1	RIPK inhibitor
2	−94.36	JTE-907	Cannabinoid receptor inverse agonist
3	−94	Rhapontin	Apoptosis stimulant
4	−93.8	Rucaparib	PARP inhibitor
5	−93.08	Nimetazepam	GABA receptor agonist
6	−92.64	RHO-kinase-inhibitor-III[rockout]	Rho associated kinase inhibitor
7	−92.35	HA-14-1	BCL inhibitor
8	−91.62	Liothyronine	Thyroid hormone stimulant
9	−90.51	Alimemazine	Histamine receptor agonist
10	−90.31	PD-173074	FGFR inhibitor

Discussion

An increasing number of studies now confirm the link between TBI and PD. Research increasingly regards TBI not only as an acute injury but also as a chronic condition.[41] TBI has been identified as a risk factor for Parkinson's disease.[10–12,42,43] Identifying the pathogenic factors linking TBI to PD is crucial for advancing clinical treatments for TBI and implementing effective preventive strategies for PD. Our study is the first to elucidate the critical role of GPX3 in traumatic brain injury (TBI)-associated Parkinson's disease (PD), highlighting its potential as a novel therapeutic target.

In this study, we analyzed two microarray datasets from TBI and PD with bioinformatics methods, identifying 20 common DEGs for TBI and PD using the GEO database. According to GO and KEGG analysis, the 912 DEGs for TBI were primarily enriched in pathways related to ribosomes, mitochondrial activation, amino acid metabolism, and neurodegenerative diseases. The 718 DEGs for PD were mainly enriched in neuronal activity, mitochondrial activation, immune cell infiltration and differentiation, and the PI3K-Akt signaling pathway. The mitochondrial activation pathway is enriched in the DEGs of both TBI and PD, with numerous studies confirming its role in PD pathogenesis.[44] Mitochondrial dysfunction is considered central to the mechanisms underlying both sporadic and familial PD. Observations from experimental models and human PD cases provide strong evidence of disrupted mitochondrial dynamics, bioenergetic deficits, inhibition of complex I in the electron transport chain (ETC), and increased reactive oxygen species (ROS).[45–47]

Additionally, by identifying co-expressed genes between TBI and PD, we found 10 commonly upregulated genes and 10 commonly downregulated genes. The upregulated genes were primarily enriched in the hypoxia pathway, while the downregulated genes were mainly enriched in pathways related to hydrogen peroxide catabolism, metabolism, and cellular oxidant detoxification. The co-expressed genes are enriched in the hypoxia pathway and the hydrogen peroxide metabolic process, which are closely related. Hypoxic conditions affect cellular redox balance, leading to increased production of reactive oxygen species (ROS), among which hydrogen peroxide (H_2O_2) is a key ROS.[48–52]

Primary brain injury generates significant amounts of ROS in mitochondria.[53] Excessive ROS leads to oxidative neuronal damage, contributing to several forms of neuronal cell death, including ferroptosis (42,43). Persistent ROS production drives neuroinflammation, which further damages the brain (44,45). Neuroinflammation increases blood-brain barrier (BBB) permeability, enabling immune cell infiltration in the ischemic brain. Cytokines produced during neuroinflammation, such as IL-1 and IL-6, exacerbate the inflammatory response.[54,55] In TBI, external impact causes mechanical damage that elevates ROS levels at the injury site.[56,57] Excessive ROS damages subcellular structures, particularly mitochondria, triggering inflammatory responses.[56] These conditions severely impact the daily lives of patients, and no effective treatments are currently available.[58]

Subsequently, we conducted a PPI network analysis, visualized using Cytoscape, and identified key hub genes, including GPX3 and CXCR4. Transcription factors (TFs) contribute significantly to gene expression regulation. In this study, we used NetworkAnalyst 3.0 to identify transcription factors associated with hub genes. In the TF-gene interaction network, GPX3, MAFF, and CLDN15 exhibited extensive connections with other TFs, while WRNA1, ZFP37, and IKZF1 were the most active transcription factors. IKZF1 (Ikaros family zinc finger 1) is a zinc finger protein of the Ikaros

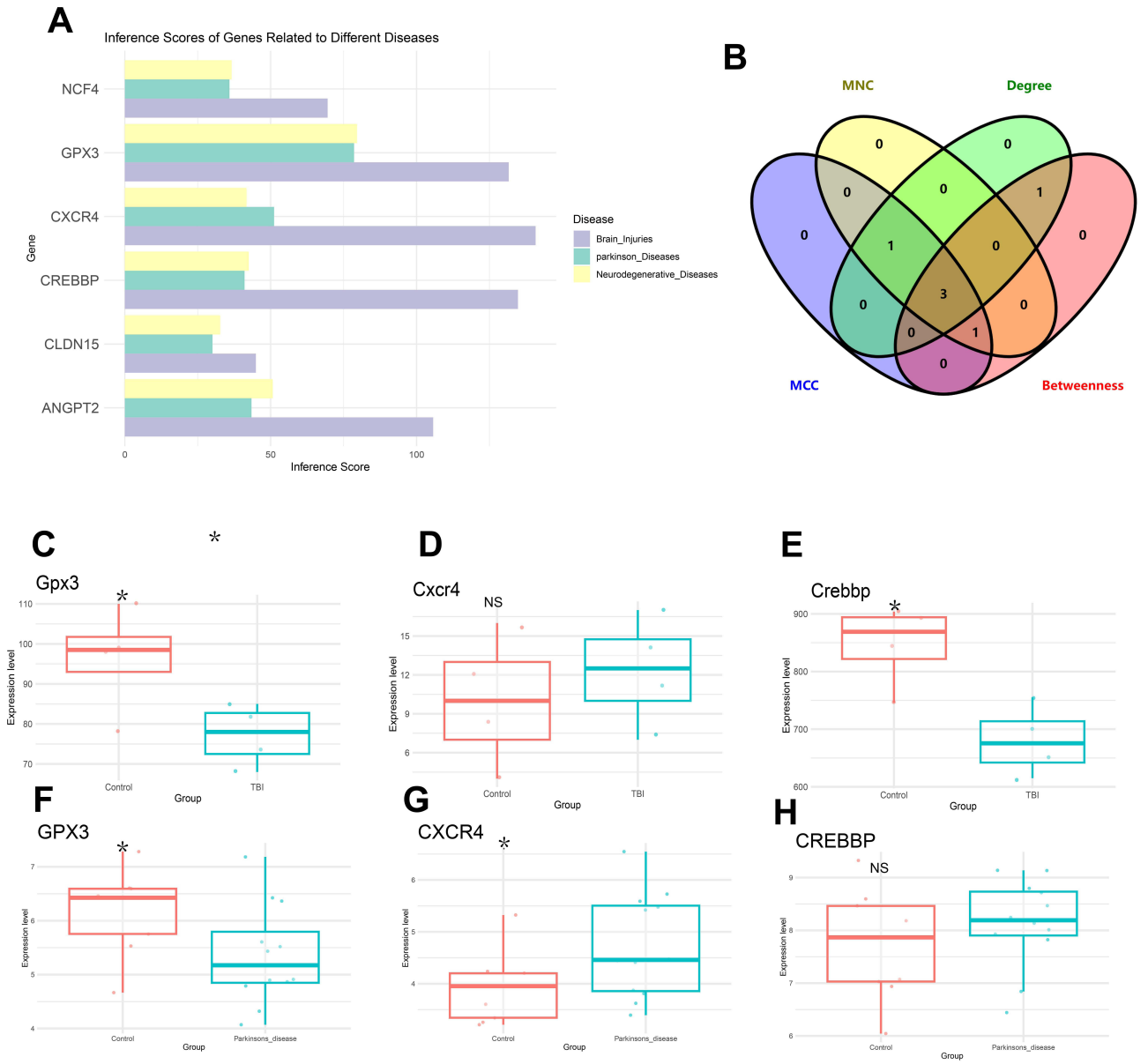

Figure 7 Dataset Validation of Hub Genes. (**A**). Analysis of the relationship between hub genes and brain injuries, Parkinson's disease, and other neurodegenerative diseases based on the Comparative Toxicogenomics Database (CTD). (**B**). Identification of the three hub genes using four algorithms (MCC, MNC, degree, and Betweenness) of the CytoHubba plugin in Cytoscape. (**C**). Expression of Gpx3 in the validation dataset GSE150696. (**D**). Expression of Cxcr4 genes in the validation dataset GSE150696. (**E**). Expression of Crebbp genes in the validation dataset GSE150696. (**F**). Expression of GPX3 genes in the validation dataset GSE155063. (**G**). Expression of CXCR4 genes in the validation dataset GSE155063. (**H**). Expression of CREBBP genes in the validation dataset GSE155063.
Notes: *P < 0.05 Statistical analysis was performed using Student's *t*-test.

family, playing a crucial role in the development and function of the immune system.[59,60] It is widely recognized as an important transcription factor regulating the development, differentiation, and expression of immune-related genes in lymphocytes.[61,62]

Small noncoding RNAs known as miRNAs (21–25 nucleotides in length) can complement the 3′ UTR of target mRNAs, resulting in either mRNA degradation or translational inhibition.[63] In the constructed mRNA-miRNA regulatory network, miR-548-3p, miR-653, miR-543, and miR-340 showed the highest average connectivity. These miRNAs are critical regulators in cancer and immune response pathways. miR-548-3p is primarily involved in cell cycle and immune regulation, with tumor-suppressive properties in cancer.[64] miR-653 plays a key role in inflammation and immune modulation, particularly in autoimmune diseases and cancer.[65] miR-543 controls tumor cell proliferation and

https://doi.org/10.2147/JIR.S506891

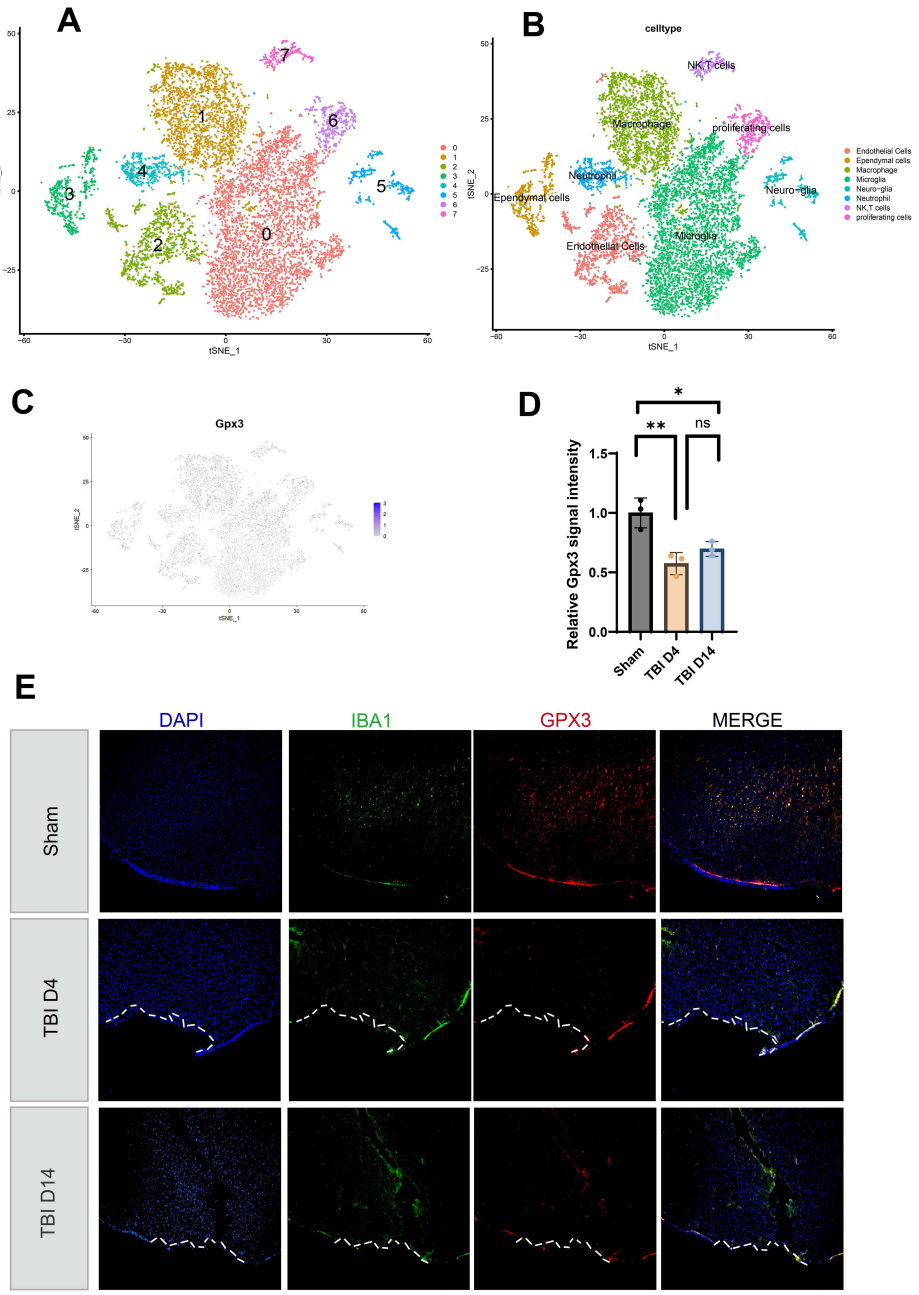

Figure 8 Single-Cell Dataset Overview and Experimental Validation of Gpx3. (**A**). t-SNE clustering of cells reveals distinct cell populations based on transcriptome data. (**B**). Annotation of cell clusters into eight categories: endothelial cells, ependymal cells, macrophages, microglia, neuroglia, neutrophils, NK/T cells, and proliferating cells. (**C**). Expression levels of Gpx3 across cell populations, with color intensity indicating expression levels in each cell type. (**D**). Quantitative analysis of the relative fluorescence intensity of Gpx3 in brain sections from the sham-operated group and at days 4 and 14 post-TBI(n=3). Statistical significance was assessed using one-way ANOVA followed by Tukey's post hoc test for multiple comparisons. Data are presented as mean ± SEM. *, $p<0.05$, **, $p < 0.01$ (**E**). Representative immunofluorescence images of brain sections from the sham-operated group and mice at days 4 and 14 post-TBI. DAPI (blue) marks nuclei, IBA1 (green) labels microglia, and Gpx3 (red) shows the distribution of Gpx3 protein. The dashed white line indicates the cortical boundary.

Abbreviations: TBI, traumatic brain injury; PD, Parkinson's disease; DEG, differentially expressed genes; PPI, protein-protein interaction; CTD, Comparative Toxicogenomics Database; CCI, controlled cortical impact; CNS, central nervous system; ENS, enteric nervous system; GI, gastrointestinal; GO, Gene Ontology; KEGG, Kyoto Encyclopedia of Genes and Genomes; ROS reactive oxygen species; BBB, blood-brain barrier; TF, Transcription factor.

invasion by targeting cancer-related genes, with additional roles in cardiovascular and neurological diseases.[66] miR-340 functions as a tumor suppressor, regulating cancer cell proliferation and inflammatory responses, demonstrating protective effects in immune-related diseases.[67] Collectively, these miRNAs contribute significantly to cell proliferation, immune response, and inflammation through targeted gene regulation.

Using the cMAP database, we identified drugs with potential efficacy for treating TBI-related Parkinson's disease, including Necrostatin-1, JTE-907, rhapontin. For validation, we further used the CTD database and an additional TBI and PD dataset from GEO, confirming that GPX3 also showed consistent results in the validation dataset. Finally, we analyzed a single-cell dataset from IBD samples for single-cell annotation analysis, finding that GPX3 and CXCR4 genes were mainly localized in microglia and macrophages, while CREBBP showed no specific distribution preference. In immunofluorescence validation in CCI model TBI mice, GPX3 expression was decreased in the cortex post-TBI, with predominant co-expression of GPX3 and IBA1. This confirmed the critical role of GPX3 in microglia and macrophages in the pathology of TBI.

GPX3 is the most promising gene in our study. Glutathione peroxidases are well-known antioxidant enzymes that catalyze the reduction of hydrogen peroxide or organic hydroperoxides using glutathione. Among the eight reported GPXs, GPX3 is a highly conserved protein and serves as the primary ROS scavenger in plasma.[21,22,68] GPX3 is an important antioxidant enzyme in the human body, responsible for clearing ROS and protecting cells from oxidative damage. However, research on the role of GPX3 in TBI and PD is limited, presenting an avenue for future investigation. As a key antioxidant enzyme, GPX3 plays a central role in various antioxidant defense mechanisms.[21] While basic research in recent years has highlighted the potential of GPX3 in various diseases, the translation of these findings into clinical applications remains limited.[69] Currently, no suitable drugs or agonists are available that can directly induce GPX3 expression.[21,69] Additionally, potential off-target effects of GPX3-based treatment strategies must not be overlooked.

We hypothesize that the increased incidence of PD following TBI may partly result from reduced GPX3 expression in injured brain tissue, causing elevated ROS levels that promote PD-related pathology. Our analyses strongly indicate the significant role of GPX3 and ROS in TBI-associated PD.

This study is limited by data and sample restrictions. Specifically, it relied solely on data obtained from TBI or PD patients, rather than from patients with both conditions. Additionally, we were unable to obtain brain tissue samples from PD patients with a history of TBI to verify the expression of key genes. Future studies should collect brain tissue samples from PD patients with a history of TBI to further investigate the relationship between TBI and PD. Furthermore, due to limited funding and experimental constraints, this study lacks functional experiments on GPX3 in TBI and PD, including the effects of GPX3 knockout or knockdown on these conditions, which diminishes the persuasiveness of the findings. We hope that future studies will address these limitations.

Conclusion

We evaluated transcriptomic data from TBI and PD patients, identifying common DEGs and hub genes shared by both conditions, and conducted a series of downstream analyses. Our findings suggest that the increased risk of PD following TBI may be driven by excessive ROS production and impaired clearance, with the GPX3 gene playing a key role in this process. These insights offer a novel perspective that may inform the prevention and treatment of TBI-related PD in the future.

Data Sharing Statement

The three datasets (GSE104687, GSE7621, GSE150696) analyzed in this study can be found in NCBI Gene Expression Omnibus (GEO).

Ethical Statement

The study was approved by the Animal Ethics Committee of the Department of Laboratory Animal Science, Fudan University (Approval number: 2021JS −342). The human data used in the public databases in this study are exempt from ethical review according to Items 1 and 2 of Article 32 of the Measures for Ethical Review of Life Sciences and Medical Research Involving Human Subjects(2023, China).

Acknowledgments

We thank the databases and software mentioned above for providing us with data and analysis tools.

Funding

This work was supported by the Science and Technology Commission of Shanghai Municipality (Grant No. 21002411700 to J.Y.).

Disclosure

The authors report no conflicts of interest concerning the materials or methods used in this study or the findings specified in this paper.

References

1. Millis SR, Rosenthal M, Novack TA, et al. Long-term neuropsychological outcome after traumatic brain injury. *J Head Trauma Rehabil*. 2001;16:343. doi:10.1097/00001199-200108000-00005
2. Huijben JA, Wiegers EJA, Lingsma HF, et al. Changing care pathways and between-center practice variations in intensive care for traumatic brain injury across Europe: a CENTER-TBI analysis. *Intensive Care Med*. 2020;46:995–1004. doi:10.1007/s00134-020-05965-z
3. Samuels JM, Moore EE, Silliman CC, et al. Severe traumatic brain injury is associated with a unique coagulopathy phenotype. *J Trauma Acute Care Surg*. 2019;86:686. doi:10.1097/TA.0000000000002173
4. Perry DC, Sturm VE, Peterson MJ, et al. Association of traumatic brain injury with subsequent neurological and psychiatric disease: a meta-analysis. *J Neurosurg*. 2016;124:511–526. doi:10.3171/2015.2.JNS14503
5. Maas AIR, Menon DK, Manley GT, et al. Traumatic brain injury: progress and challenges in prevention, clinical care, and research. *Lancet Neurol*. 2022;21:1004–1060. doi:10.1016/S1474-4422(22)00309-X
6. Masel BE, DeWitt DS. Traumatic brain injury: a disease process, not an event. *J Neurotrauma*. 2010;27:1529–1540.
7. Tolosa E, Garrido A, Scholz SW, Poewe W. Challenges in the diagnosis of Parkinson's disease. *Lancet Neurol*. 2021;20:385–397. doi:10.1016/S1474-4422(21)00030-2
8. Poewe W, Seppi K, Tanner CM, et al. Parkinson disease. *Nat Rev Dis Primers*. 2017;3:1–21. doi:10.1038/nrdp.2017.13
9. Costa HN, Esteves AR, Empadinhas N, Cardoso SM. Parkinson's disease: a multisystem disorder. *Neurosci Bull*. 2023;39:113–124. doi:10.1007/s12264-022-00934-6
10. Brett BL, Gardner RC, Godbout J, Dams-O'Connor K, Keene CD. Traumatic brain injury and risk of neurodegenerative disorder. *Biol Psychiatry*. 2022;91:498–507. doi:10.1016/j.biopsych.2021.05.025
11. Balabandian M, Noori M, Lak B, Karimizadeh Z, Nabizadeh F. Traumatic brain injury and risk of Parkinson's disease: a meta-analysis. *Acta Neurol Belg*. 2023;123:1225–1239. doi:10.1007/s13760-023-02209-x
12. Delic V, Beck KD, Pang KCH, Citron BA. Biological links between traumatic brain injury and Parkinson's disease. *Acta Neuropathol Commun*. 2020;8(45). doi:10.1186/s40478-020-00924-7
13. Raj R, Kaprio J, Korja M, et al. Risk of hospitalization with neurodegenerative disease after moderate-to-severe traumatic brain injury in the working-age population: a retrospective cohort study using the Finnish national health registries. *PLoS Med*. 2017;14:e1002316. doi:10.1371/journal.pmed.1002316
14. Gardner RC, Byers AL, Barnes DE, et al. Mild TBI and risk of Parkinson disease. *Neurology*. 2018;90:e1771–e1779. doi:10.1212/WNL.0000000000005522
15. Kohchi C, Inagawa H, Nishizawa T, Soma G-I. ROS and innate immunity. *Anticancer Res*. 2009;29:817–821.
16. Chen Y, Zhou Z, Min W. Mitochondria, Oxidative Stress and Innate Immunity. *Front Physiol*. 2018;9. doi:10.3389/fphys.2018.01487
17. Dreher D, Junod AF. Role of oxygen free radicals in cancer development. *Eur J Cancer*. 1996;32:30–38. doi:10.1016/0959-8049(95)00531-5
18. Cooke MS, Evans MD, Dizdaroglu M, Lunec J. Oxidative DNA damage: mechanisms, mutation, and disease. *THE FASEB Journal*. 2003;17:1195–1214. doi:10.1096/fj.02-0752rev
19. Kunsch C, Medford RM. Oxidative stress as a regulator of gene expression in the vasculature. *Circ Res*. 1999;85:753–766. doi:10.1161/01.RES.85.8.753
20. Zhu X, Wang J, Li L, et al. GPX3 suppresses tumor migration and invasion via the FAK/AKT pathway in esophageal squamous cell carcinoma. *Am J Transl Res*. 2018;10:1908–1920.
21. Nirgude S, Choudhary B. Insights into the role of GPX3, a highly efficient plasma antioxidant, in cancer. *Biochem. Pharmacol*. 2021;184:114365. doi:10.1016/j.bcp.2020.114365
22. Chang C, Worley BL, Phaëton R, Hempel N. Extracellular glutathione peroxidase GPx3 and its role in cancer. *Cancers*. 2020;12:2197. doi:10.3390/cancers12082197
23. Mills GC. Hemoglobin catabolism: i. Glutathione peroxidase, an erythrocyte enzyme which protects hemoglobin from oxidative breakdown. *J Biol Chem*. 1957;229:189–197. doi:10.1016/S0021-9258(18)70608-X
24. Brigelius-Flohé R, Maiorino M. Glutathione peroxidases. *Biochimica et Biophysica Acta*. 2013;1830:3289–3303. doi:10.1016/j.bbagen.2012.11.020
25. Barrett CW, Ning W, Chen X, et al. Tumor suppressor function of the plasma glutathione peroxidase Gpx3 in colitis-associated carcinoma. *Cancer Res*. 2013;73:1245–1255. doi:10.1158/0008-5472.CAN-12-3150
26. Mohamed MM, Sabet S, Peng D-F, et al. Promoter hypermethylation and suppression of Glutathione Peroxidase 3 are associated with inflammatory breast carcinogenesis. *Oxid Med Cell Longev*. 2014;2014:787195. doi:10.1155/2014/787195
27. Miller JA, Guillozet-Bongaarts A, Gibbons LE, et al. Neuropathological and transcriptomic characteristics of the aged brain. *eLife*. 2017;6:e31126. doi:10.7554/eLife.31126
28. Lesnick TG, Papapetropoulos S, Mash DC, et al. A genomic pathway approach to a complex disease: axon guidance and Parkinson disease. *PLoS Genet*. 2007;3:e98. doi:10.1371/journal.pgen.0030098
29. Low CYB, Lee JH, Lim FTW, et al. Isoform-specific upregulation of FynT kinase expression is associated with tauopathy and glial activation in Alzheimer's disease and Lewy body dementias. *Brain Pathol*. 2021;31:253–266. doi:10.1111/bpa.12917

30. Bolte AC, Dutta AB, Hurt ME, et al. Meningeal lymphatic dysfunction exacerbates traumatic brain injury pathogenesis. *Nat Commun*. 2020;11:4524. doi:10.1038/s41467-020-18113-4
31. Zhou Y, Zhou B, Pache L, et al. Metascape provides a biologist-oriented resource for the analysis of systems-level datasets. *Nat Commun*. 2019;10:1523. doi:10.1038/s41467-019-09234-6
32. Kanehisa M, Furumichi M, Tanabe M, Sato Y, Morishima K. KEGG: new perspectives on genomes, pathways, diseases and drugs. *Nucleic Acids Res*. 2017;45:D353–D361. doi:10.1093/nar/gkw1092
33. Szklarczyk D, Kirsch R, Koutrouli M, et al. The STRING database in 2023: protein-protein association networks and functional enrichment analyses for any sequenced genome of interest. *Nucleic Acids Res*. 2023;51:D638–D646. doi:10.1093/nar/gkac1000
34. Franz M, Rodriguez H, Lopes C, et al. GeneMANIA update 2018. *Nucleic Acids Res*. 2018;46:W60. doi:10.1093/nar/gky311
35. Zhou G, Soufan O, Ewald J, et al. NetworkAnalyst 3.0: a visual analytics platform for comprehensive gene expression profiling and meta-analysis. *Nucleic Acids Res*. 2019;47:W234–W241. doi:10.1093/nar/gkz240
36. Davis AP, Wiegers TC, Johnson RJ, et al. Comparative Toxicogenomics Database (CTD): update 2023. *Nucleic Acids Res*. 2023;51:D1257–D1262. doi:10.1093/nar/gkac833
37. Subramanian A, Narayan R, Corsello SM, et al. A next generation connectivity map: L1000 platform and the first 1,000,000 profiles. *Cell*. 2017;171:1437–1452.e17. doi:10.1016/j.cell.2017.10.049
38. Stuart T, Butler A, Hoffman P, et al. Comprehensive Integration of Single-Cell Data. *Cell*. 2019;177:1888–1902.e21. doi:10.1016/j.cell.2019.05.031
39. Hou W, Ji Z. Assessing GPT-4 for cell type annotation in single-cell RNA-seq analysis. *Nat Methods*. 2024;21:1462–1465. doi:10.1038/s41592-024-02235-4
40. Xiong Y, Mahmood A, Chopp M. Animal models of traumatic brain injury. *Nat Rev Neurosci*. 2013;14:128–142. doi:10.1038/nrn3407
41. Dams-O'Connor K, Juengst SB, Bogner J, et al. Traumatic brain injury as a chronic disease: insights from the United States traumatic brain injury model systems research program. *Lancet Neurol*. 2023;22:517–528. doi:10.1016/S1474-4422(23)00065-0
42. Lillian A, Zuo W, Laham L, Hilfiker S, Ye J-H. Pathophysiology and neuroimmune interactions underlying Parkinson's Disease and traumatic brain injury. *Int J mol Sci*. 2023;24:7186. doi:10.3390/ijms24087186
43. Prajjwal P, Flores Sanga HS, Acharya K, et al. Parkinson's disease updates: addressing the pathophysiology, risk factors, genetics, diagnosis, along with the medical and surgical treatment. *Ann Med Surg*. 2023;85:4887–4902. doi:10.1097/MS9.0000000000001142
44. Moradi Vastegani S, Nasrolahi A, Ghaderi S, et al. Mitochondrial dysfunction and Parkinson's Disease: pathogenesis and therapeutic strategies. *Neurochem Res*. 2023;48:2285–2308. doi:10.1007/s11064-023-03904-0
45. Ryan BJ, Hoek S, Fon EA, Wade-Martins R. Mitochondrial dysfunction and mitophagy in Parkinson's: from familial to sporadic disease. *Trends Biochem Sci*. 2015;40:200–210. doi:10.1016/j.tibs.2015.02.003
46. Winklhofer KF, Haass C. Mitochondrial dysfunction in Parkinson's disease. *Biochimica et Biophysica Acta*. 2010;1802:29–44.
47. Devi L, Raghavendran V, Prabhu BM, Avadhani NG, Anandatheerthavarada HK. Mitochondrial import and accumulation of α-synuclein impair complex I in human dopaminergic neuronal cultures and Parkinson Disease Brain *. *J Biol Chem*. 2008;283:9089–9100. doi:10.1074/jbc.M710012200
48. Tejero J, Shiva S, Gladwin MT. Sources of vascular nitric oxide and reactive oxygen species and their regulation. *Physiol Rev*. 2019;99:311–379. doi:10.1152/physrev.00036.2017
49. Bell EL, Klimova TA, Eisenbart J, Schumacker PT, Chandel NS. Mitochondrial reactive oxygen species trigger hypoxia-inducible factor-dependent extension of the replicative life span during hypoxia. *mol Cell Biol*. 2007;27:5737–5745.
50. Lee P, Chandel NS, Simon MC. Cellular adaptation to hypoxia through hypoxia inducible factors and beyond. *Nat Rev mol Cell Biol*. 2020;21:268–283.
51. Semenza GL. Hypoxia-inducible factors in physiology and medicine. *Cell*. 2012;148:399–408. doi:10.1016/j.cell.2012.01.021
52. Schieber M, Chandel NS. ROS function in redox signaling and oxidative stress. *Curr Biol*. 2014;24:R453–462.
53. Rocha EM, De Miranda B, Sanders LH. Alpha-synuclein: pathology, mitochondrial dysfunction and neuroinflammation in Parkinson's disease. *Neurobiol Dis*. 2018;109:249–257. doi:10.1016/j.nbd.2017.04.004
54. Jayaraj RL, Azimullah S, Beiram R, Jalal FY, Rosenberg GA. Neuroinflammation: friend and foe for ischemic stroke. *J Neuroinflammation*. 2019;16:142. doi:10.1186/s12974-019-1516-2
55. Candelario-Jalil E, Dijkhuizen RM, Magnus T. Neuroinflammation, stroke, blood-brain barrier dysfunction, and imaging modalities. *Stroke*. 2022;53:1473–1486. doi:10.1161/STROKEAHA.122.036946
56. Qin D, Wang J, Le A, et al. traumatic brain injury: ultrastructural features in neuronal ferroptosis, glial cell activation and polarization, and blood–brain barrier breakdown. *Cells*. 2021;10:1009. doi:10.3390/cells10051009
57. Wang J, Jiang C, Zhang K, et al. Melatonin receptor activation provides cerebral protection after traumatic brain injury by mitigating oxidative stress and inflammation via the Nrf2 signaling pathway. *Free Radic Biol Med*. 2019;131:345–355. doi:10.1016/j.freeradbiomed.2018.12.014
58. Kundu S, Singh S. What happens in TBI? A wide talk on animal models and future perspective. *Curr Neuropharmacol*. 2023;21:1139–1164. doi:10.2174/1570159X20666220706094248
59. Foà R, Bassan R, Vitale A, et al. Dasatinib-Blinatumomab for Ph-Positive Acute Lymphoblastic Leukemia in Adults. *N Engl J Med*. 2020;383:1613–1623. doi:10.1056/NEJMoa2016272
60. John LB, Ward AC. The Ikaros gene family: transcriptional regulators of hematopoiesis and immunity. *Mol Immunol*. 2011;48:1272–1278. doi:10.1016/j.molimm.2011.03.006
61. Ng SY-M, Yoshida T, Georgopoulos K. Ikaros and chromatin regulation in early hematopoiesis. *Curr Opin Immunol*. 2007;19:116–122. doi:10.1016/j.coi.2007.02.014
62. Ichiyama K, Long J, Kobayashi Y, et al. Transcription factor Ikzf1 associates with Foxp3 to repress gene expression in Treg cells and limit autoimmunity and anti-tumor immunity. *Immunity*. 2024;57:2043–2060.e10. doi:10.1016/j.immuni.2024.07.010
63. Achkar NP, Cambiagno DA, Manavella PA. miRNA Biogenesis: a Dynamic Pathway. *Trends Plant Sci*. 2016;21:1034–1044. doi:10.1016/j.tplants.2016.09.003
64. Shi Y, Qiu M, Wu Y, Hai L. MiR-548-3p functions as an anti-oncogenic regulator in breast cancer. *Biomed. Pharmacother*. 2015;75:111–116. doi:10.1016/j.biopha.2015.07.027

65. Zhang Q, Wang G, Xu B. Brucine alleviates fibroblast-like synoviocytes dysfunction and inflammation by regulating YY1 during rheumatoid arthritis. *Chem Biol Drug Des*. 2024;103:e14472. doi:10.1111/cbdd.14472
66. Wang L-H, Tsai H-C, Cheng Y-C, et al. CTGF promotes osteosarcoma angiogenesis by regulating miR-543/angiopoietin 2 signaling. *Cancer Lett*. 2017;391:28–37. doi:10.1016/j.canlet.2017.01.013
67. Herman AB, Anerillas C, Harris SC, et al. Reduction of lamin B receptor levels by miR-340-5p disrupts chromatin, promotes cell senescence and enhances senolysis. *Nucleic Acids Res*. 2021;49:7389–7405. doi:10.1093/nar/gkab538
68. Gong Y, Yang J, Cai J, et al. Effect of Gpx3 gene silencing by siRNA on apoptosis and autophagy in chicken cardiomyocytes. *J Cell Physiol*. 2019;234:7828–7838. doi:10.1002/jcp.27842
69. Zhang N, Liao H, Lin Z, Tang Q. Insights into the Role of Glutathione Peroxidase 3 in Non-Neoplastic Diseases. *Biomolecules*. 2024;14:689. doi:10.3390/biom14060689